

## INTERACTION BETWEEN AMMONIUM PERCHLORATE AND RDX

Jeffrey J. Kay<sup>1</sup>, Gary L. Biggs<sup>2</sup>, Heather F. Hayden<sup>2</sup>, and Wade G. Babcock<sup>2</sup>

<sup>1</sup> Sandia National Laboratories, Livermore, CA

<sup>2</sup> Naval Surface Warfare Center at Indian Head, Indian Head, MD

### ABSTRACT

The interaction between ammonium perchlorate and RDX at elevated temperatures is examined using Simultaneous Thermogravimetric Modulated Beam Mass Spectrometry (STMBMS). STMBMS testing indicates that at moderate temperatures ( $>150^{\circ}\text{C}$ ), RDX and ammonium perchlorate undergo a strong and unusual reaction that results in rapid and complete decomposition of RDX. The presence of ammonium perchlorate and/or its decomposition products appears to initiate catalytic decomposition of RDX.

### INTRODUCTION

Understanding the thermal response and aging characteristics of explosive and propellant formulations requires an understanding of the basic chemical reactions that occur in these materials in response to elevated temperatures. We recently described [1] the results of a campaign to quantify thermally-induced chemical changes in PBXN-111, an underwater explosive formulation (whose primary ingredients include the common ingredients ammonium perchlorate, RDX, and aluminum), with the goal of identifying chemical changes that could take place at or near ambient temperatures and potentially affect the aging characteristics of the formulation. Part of that work involved determining whether chemical reactions take place between pairs of ingredients of the formulation at elevated temperatures. Using Simultaneous Thermogravimetric Modulated Beam Mass Spectrometry (STMBMS) [2-4], we observed and characterized a very clear chemical interaction between ammonium perchlorate and RDX that occurs at temperatures of approximately  $150^{\circ}\text{C}$  and above. The reaction results in complete and rapid decomposition of RDX, occurs promptly upon melting point of RDX, occurs with variable delay below the melting point of RDX, and does not significantly consume the ammonium perchlorate. This unusual reaction is investigated and characterized in this paper.

### EXPERIMENT

#### STMBMS APPARATUS

Simultaneous Thermogravimetric Modulated Beam Mass Spectrometry (STMBMS) [2-4] was used to investigate the thermal decomposition chemistry of ammonium perchlorate (AP), RDX, and AP/RDX mixtures at moderate temperatures. References [2] – [7] describe the experimental methods and numerical algorithms used to examine and characterize the reactions of energetic materials at elevated temperatures. The basic features of a thermal decomposition experiment using the STMBMS instrument are illustrated in Figure 1. A small sample of energetic material (ingredient or mixture; 2-15 mg) is placed in an alumina reaction cell (free volume of  $0.227 \text{ cm}^3$ ), which is sealed with a cap assembly containing a ceramic cup with a  $5\text{-}1000\mu\text{m}$  orifice at its center. The reaction cell is heated in a controlled manner using a thermocouple and programmable thermal controller to measure and control the temperature of the cell. As the

reaction cell is heated, gaseous compounds are generated due to thermal decomposition of the sample. These gases fill the free volume of the reaction cell, causing it to pressurize. The pressurized gas flows through the orifice and expands into vacuum, forming a molecular beam. The resulting molecular beam is directed into a quadrupole mass spectrometer, where the relative abundance of each constituent is measured. The reaction cell sits atop a microbalance, which records the change in mass of the sample as it is heated and undergoes sublimation/evaporation and decomposition. Together these measurements allow identification and determination of the time-and temperature-dependent rate of formation of each gaseous species that evolves from the heated sample.

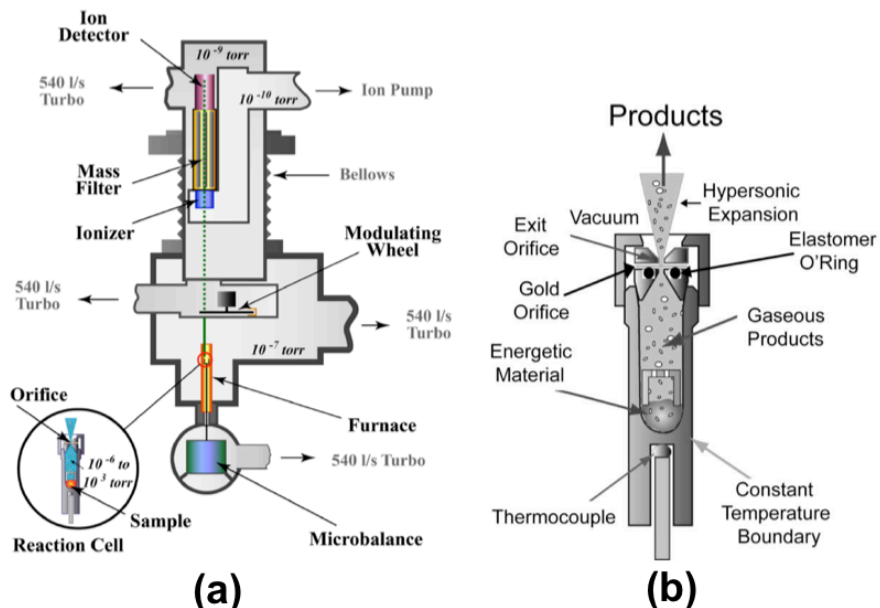


**Figure 1. (a) Schematic diagram of the Simultaneous Thermogravimetric Modulated Beam Mass Spectrometry (STMBMS) instrument. (b) Schematic diagram of the reaction cell illustrating a typical sample configuration used in an STMBMS experiment.**

The pressure of gases within the reaction cell is determined by the diameter of the orifice and the experimental conditions. The gas pressure within the cell is determined by a steady-state balance between the rate of gas formation from the sample and the rate of exhaust through the orifice. Smaller orifices will produce higher pressures for a given gas formation rate from the sample. For compounds in two-phase quasi-equilibrium, the pressure is determined by the temperature of the reaction cell and the properties of the compounds. In this case, a smaller orifice results in less of the gas exiting the reaction cell. The reaction conditions are controlled by altering the sample size, temperature, heating rate, orifice diameter and volume of the reaction cell.

## SAMPLES

Samples of ammonium perchlorate and RDX were received from NSWC Indian Head Explosive Ordnance Disposal Technology Division (NSWC IHEODTD). The ammonium perchlorate powder consists of  $\sim 200$   $\mu\text{m}$  diameter particles and contains 0.2% tricalcium phosphate. The RDX powder (Class 5), contains up to 15% HMX. Samples of AP and RDX were used as received, and AP/RDX mixtures were prepared by manual stirring without additional treatment.

## RESULTS AND DISCUSSION

The thermal decomposition chemistry of both ammonium perchlorate and RDX have been thoroughly investigated previously [8-11]. At temperatures 130°C – 240°C, AP undergoes partial decomposition to produce ammonia (NH<sub>3</sub>), perchloric acid (HClO<sub>4</sub>), H<sub>2</sub>O, O<sub>2</sub>, HCl, Cl<sub>2</sub>, NO<sub>2</sub>, and N<sub>2</sub>O. The decomposition mechanism is shown in Figure xx. Dissociative sublimation (**R1**) to produce NH<sub>3</sub> and HClO<sub>4</sub> occurs in tandem with decomposition of the solid (**R2**) to produce H<sub>2</sub>O, O<sub>2</sub>, HCl, Cl<sub>2</sub>, NO<sub>2</sub>, and N<sub>2</sub>O. Under low confinement, dissociative sublimation (**R1**) and solid phase decomposition (**R2**) govern the decomposition kinetics; under high confinement, gas/surface (**R3**) and gas-phase (**R4**) reactions also participate. Below 240°C, the solid only partially decomposes, generating the above gas phase species and leaving behind a microporous solid consisting of pure ammonium perchlorate. At higher temperatures, decomposition is complete.

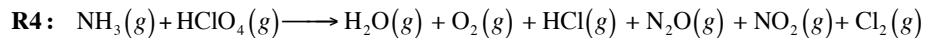
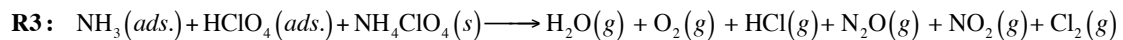
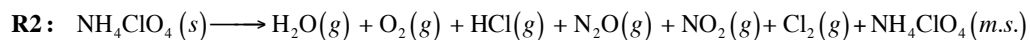
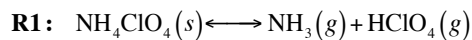


**Figure 1. Thermal decomposition mechanism of ammonium perchlorate.**

STMBMS data for thermal decomposition of AP are shown in Figures 2 and 3. Figure 2 shows data obtained during thermal decomposition of AP under low confinement, and Figure 3 shows data obtained for thermal decomposition of AP under high confinement. In both experiments, AP is heated from ambient temperature to 500°C at a rate of 2°C/min. Mass loss curves and representative mass spectrum signals for NH<sub>3</sub> and HClO<sub>4</sub>, H<sub>2</sub>O, O<sub>2</sub>, and Cl<sub>2</sub> are shown for both cases. Under low confinement, AP begins to decompose rapidly at 220°C and continues until the sample is fully depleted. Under high confinement, AP undergoes rapid solid phase decomposition above 260°C, with gas and gas/surface reactions participating above 320°C, giving rise to two distinct mass loss phases and two maxima in the H<sub>2</sub>O, O<sub>2</sub>, and Cl<sub>2</sub> ion signals.

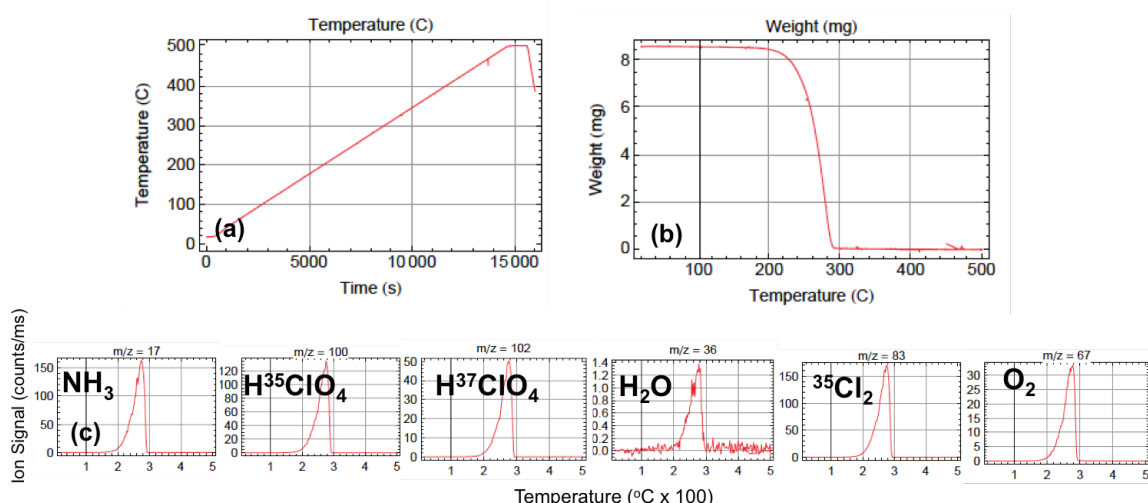


**Figure 2. STMBMS data from thermal decomposition of AP under low confinement. (a) Thermal profile. (b) Weight loss. (c) Mass spectrum data.**

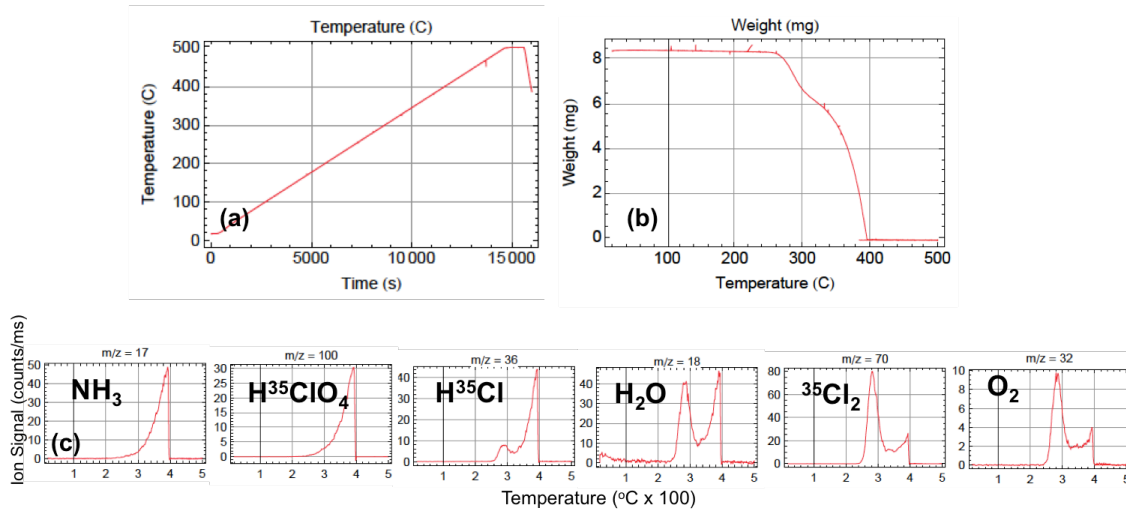


**Figure 3. STMBMS data from thermal decomposition of AP under high confinement. (a) Thermal profile. (b) Weight loss. (c) Mass spectrum data.**

The thermal decomposition mechanism of RDX is complex and will only be summarized here. RDX decomposes both below and above its melting point, with liquid-phase decomposition being more rapid. The decomposition process is autocatalytic, with the decomposition products accelerating decomposition of unreacted RDX. Below its melting point, RDX decomposes by gas and gas-surface reactions to produce a variety of products, including formaldehyde ( $\text{CH}_2\text{O}$ ),  $\text{N}_2\text{O}$ ,  $\text{NO}$ ,  $\text{NO}_2$ ,  $\text{N}_2$ , and  $\text{H}_2\text{O}$ . Above its melting point, RDX decomposes by a set of reactions to produce similar products. In both cases, a nonvolatile residue (NVR) consisting of high-molecular-weight decomposition products forms. The decomposition process below and above the melting point are accelerated by the decomposition products; in particular  $\text{NO}$  and the NVR. The decomposition mechanism is shown in Figures 4 and 5. STMBMS data for thermal decomposition of RDX are shown in Figures 6 and 7. Figure 6 shows STMBMS data for thermal decomposition of RDX under low confinement, and Figure 7 shows data for thermal decomposition of RDX under high confinement. In both experiments, RDX is heated from ambient temperature to  $240^\circ\text{C}$  at a rate of  $2^\circ\text{C}/\text{min}$ . In the low confinement experiment, RDX (and the HMX impurity) undergo rapid sublimation without appreciable decomposition. RDX sublimation occurs between  $120$ - $170^\circ\text{C}$ , and HMX sublimation occurs between  $170$ - $220^\circ\text{C}$ , giving rise to two sequential mass loss steps and two peaks in the mass spectrum data. In the high confinement experiment, evaporation of RDX is observed above  $\sim 160^\circ\text{C}$ , and the sample primarily undergoes decomposition upon melting, at approximately  $185^\circ\text{C}$ , and completes decomposition approximately 2000 seconds later. Figure 7 shows mass spectrum signals for RDX as well as  $\text{CH}_2\text{O}$ ,  $\text{N}_2\text{O}$ , oxy-s-triazine, and  $N,N$ -dimethylformamide, which are all liquid-phase decomposition products.

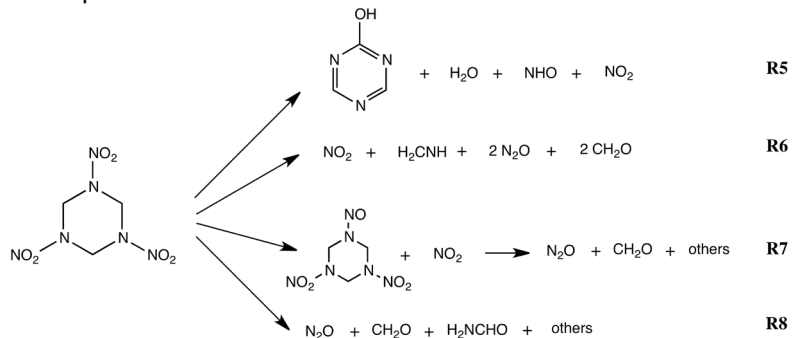


**Figure 4. Thermal decomposition mechanism for RDX above its melting point.**

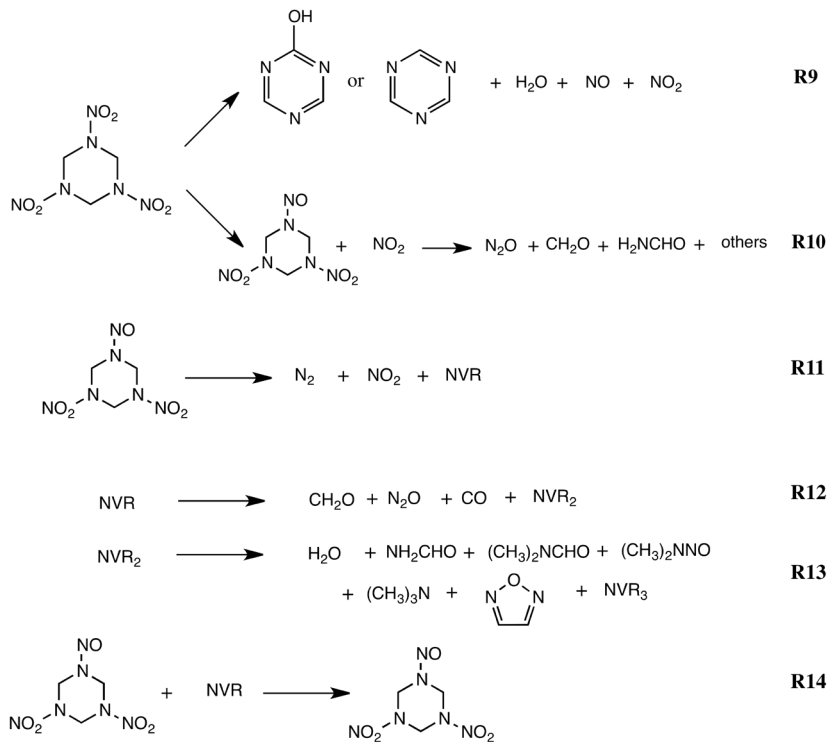


**Figure 5. Thermal decomposition mechanism for RDX below its melting point; gas phase reactions (R9 and R10) and surface reactions (R11-R14).**

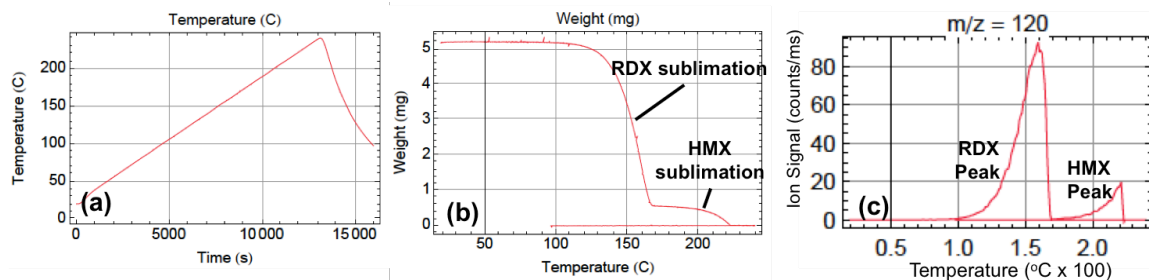


**Figure 6. STMBMS data from thermal decomposition of RDX under low confinement. (a) Temperature profile. (b) Mass loss curve. (c) Mass spectrum data, showing typical signal at  $m/z = 120$ . Both RDX and the HMX impurity produce fragments with  $m/z = 120$  in our experiments.**

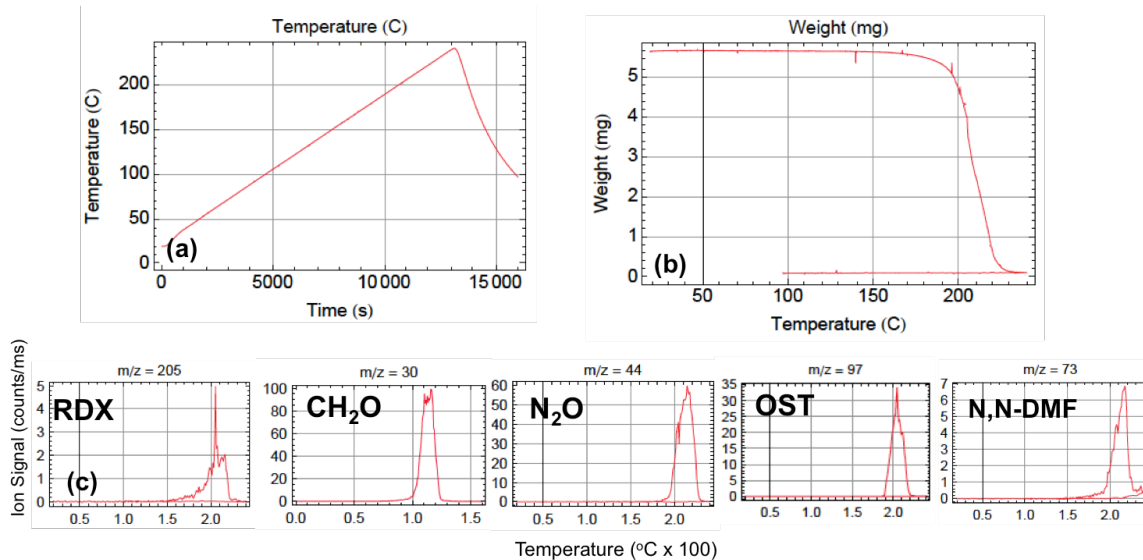


**Figure 7. STMBMS data from thermal decomposition of RDX under high confinement. (a)** Temperature profile. **(b)** Mass loss curve. **(c)** Mass spectrum data, showing signals from RDX, formaldehyde ( $\text{CH}_2\text{O}$ ),  $\text{N}_2\text{O}$ , oxy-s-triazine (OST), and  $N,N$ -dimethylformamide (DMF).  $\text{CH}_2\text{O}$  and  $\text{N}_2\text{O}$  are major decomposition products, OST is typically observed in liquid phase decomposition of RDX, and DMF is generated by the nonvolatile residue (see reaction mechanism above).

STMBMS data from thermal decomposition of an AP/RDX mixture is shown in Figure 8; optical images of the sample before and after are shown in Figure 9. In this experiment, 4.08 mg of RDX is mixed with 5.66 mg of AP, and the mixture is heated from ambient temperature to 500°C at a rate of 2°C/min under high confinement. The mass loss and mass spectrum data show a series of distinct steps. Between 120-185°C, RDX is observed to sublime from the sample. At 185°C, a rapid reaction occurs, terminating the RDX signal, giving rise to rapid mass loss (equal to the mass of RDX), and producing a short burst of decomposition products (particularly  $\text{CH}_2\text{O}$ ,  $\text{N}_2\text{O}$ , and  $\text{H}_2\text{O}$ ). Notably, a burst of HCl is also observed. The mass of the sample is then constant until ~270°C, when a second, slower decomposition step occurs, during which the remainder of the sample decomposes and produces typical AP decomposition products ( $\text{NH}_3$ ,  $\text{HClO}_4$ ,  $\text{HCl}$ ,  $\text{Cl}_2$ ,  $\text{O}_2$ , and  $\text{H}_2\text{O}$ , among others). While the second decomposition step is similar to the typical decomposition of AP under high confinement, the first step is unlike the decomposition process of RDX under the same conditions. The first decomposition step occurs in approximately 100s; 20 times faster than decomposition of RDX alone (see Fig. 7). While some of the decomposition products produced in the first step ( $\text{N}_2\text{O}$ ,  $\text{CH}_2\text{O}$ ,  $\text{H}_2\text{O}$ , and others) appear in during thermal decomposition of pure RDX, oxy-s-triazine, which is normally observed during liquid-phase decomposition of RDX, is notably absent, suggesting that the decomposition chemistry may be altered in the presence of ammonium perchlorate. The appearance of HCl during the RDX decomposition step suggests that a chemical interaction with AP may be driving the decomposition process.

STMBMS data from isothermal decomposition of an AP/RDX mixture at 170°C under high confinement is shown in Figures 10-12. In this experiment, the sample is heated from room temperature to 170°C at a rate of ~5°C/min and is held at 170°C thereafter. The sample reaches the 170°C isothermal temperature after approximately 2000s. The temperature of this experiment is below the melting point of RDX. The STMBMS data again shows two distinct steps in the decomposition process: a rapid reaction that results in complete decomposition of RDX, and a much slower reaction at later time that decomposes the AP. The RDX decomposition step begins at approximately 6,500s (4,500s after reaching 170°C) and is complete at approximately 7,000s (5,000s after reaching 170°C). The products observed during this step of the reaction again

include  $\text{CH}_2\text{O}$ ,  $\text{N}_2\text{O}$ ,  $\text{H}_2\text{O}$ , which are normally observed in RDX decomposition, along with  $\text{HCl}$ , and again without oxy-s-triazine. Although the reaction products are similar to those observed in the thermal ramp experiment shown in Figure 8, this reaction is unusual in that the rapid decomposition occurs *after a delay during which no products other than RDX (generated by sublimation of the solid) are detected*, as the sample is held at constant temperature. The decomposition observed here is in stark contrast to the decomposition of pure RDX, which decomposes very slowly below its melting point – on the timescale of tens of hours [11]. No such abrupt reaction is observed in the decomposition of pure RDX below its melting point.

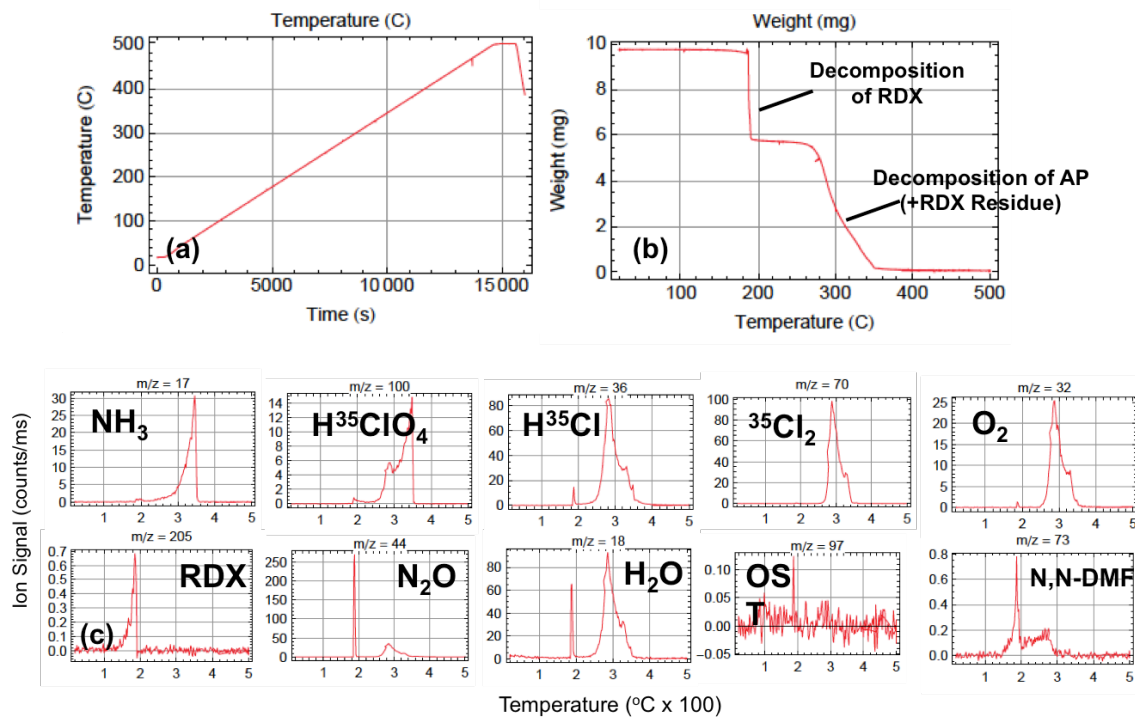


**Figure 8. STMBMS data from thermal decomposition of AP/RDX mixture. (a) Temperature profile. (b) Mass loss curve. (c) Mass spectrum data, showing signals from RDX and AP decomposition products. Decomposition proceeds in two steps, with rapid decomposition of RDX in the first step, and slower decomposition of AP in the second. Note the presence of  $\text{HCl}$  in the first reaction step, indicating chemical interaction between AP and RDX.**

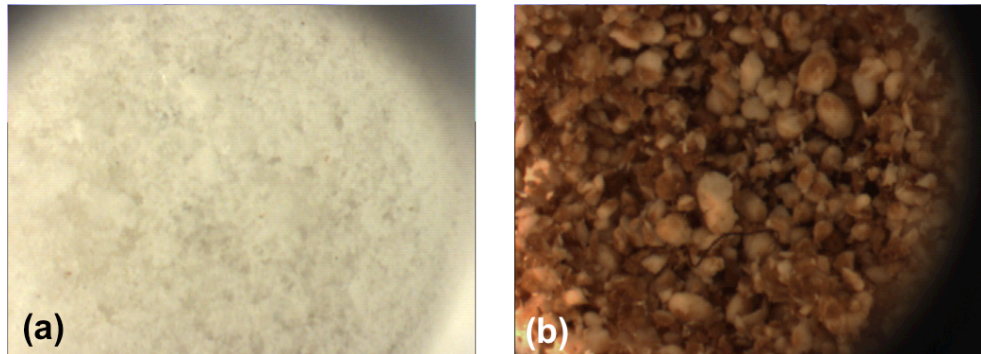


**Figure 9. Optical images of AP/RDX mixture (a) before and (b) after reaction. As the images show, the much smaller RDX particles decompose during the reaction, producing a colored residue on the surface of the ammonium perchlorate particles.**

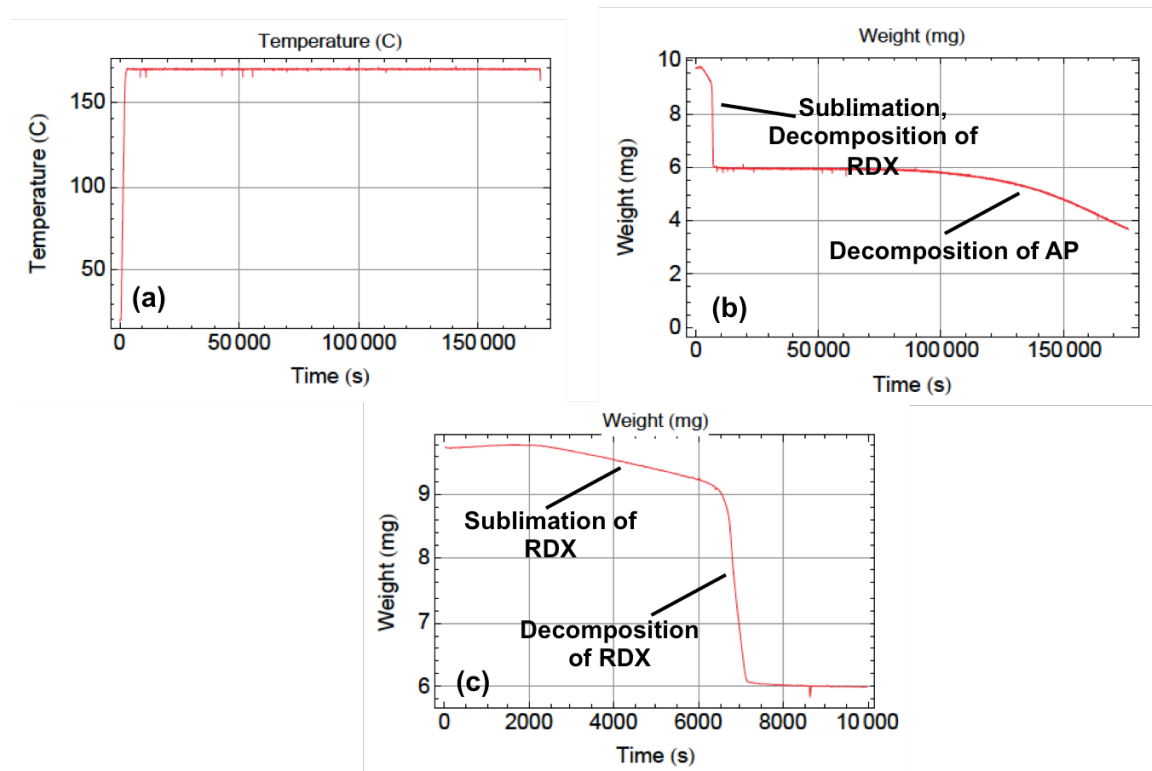


**Figure 10.** STMBMS mass loss data from isothermal decomposition of AP/RDX mixture at 170°C. (a) Temperature profile. (b) Mass loss data. (c) Mass loss data, expanded to highlight early stages of reaction where RDX decomposes rapidly.

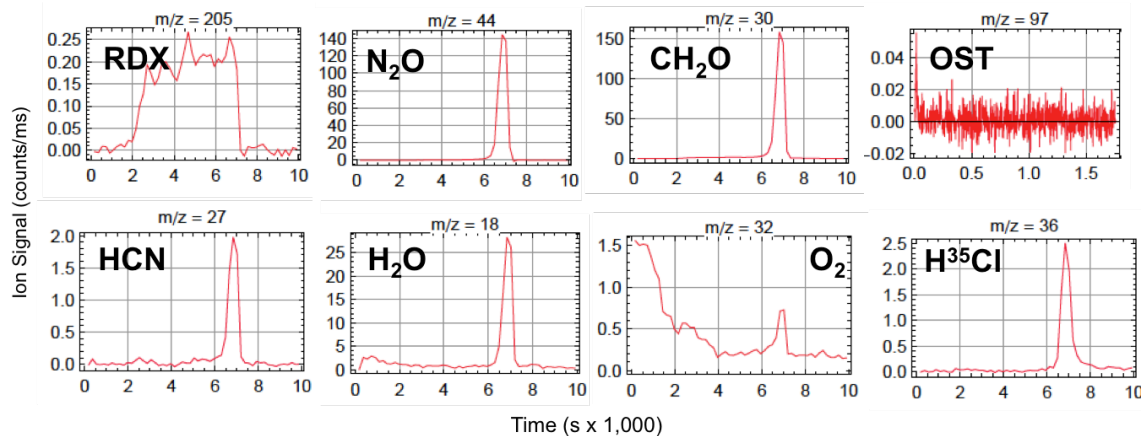


**Figure 11.** STMBMS mass spectrum data from the isothermal decomposition of AP/RDX mixture at 170°C, showing decomposition products observed in the RDX reaction step. Rapid decomposition of RDX occurs at approximately 6,500s, generating CH<sub>2</sub>O, N<sub>2</sub>O, HCN, and other decomposition products, along with HCl.

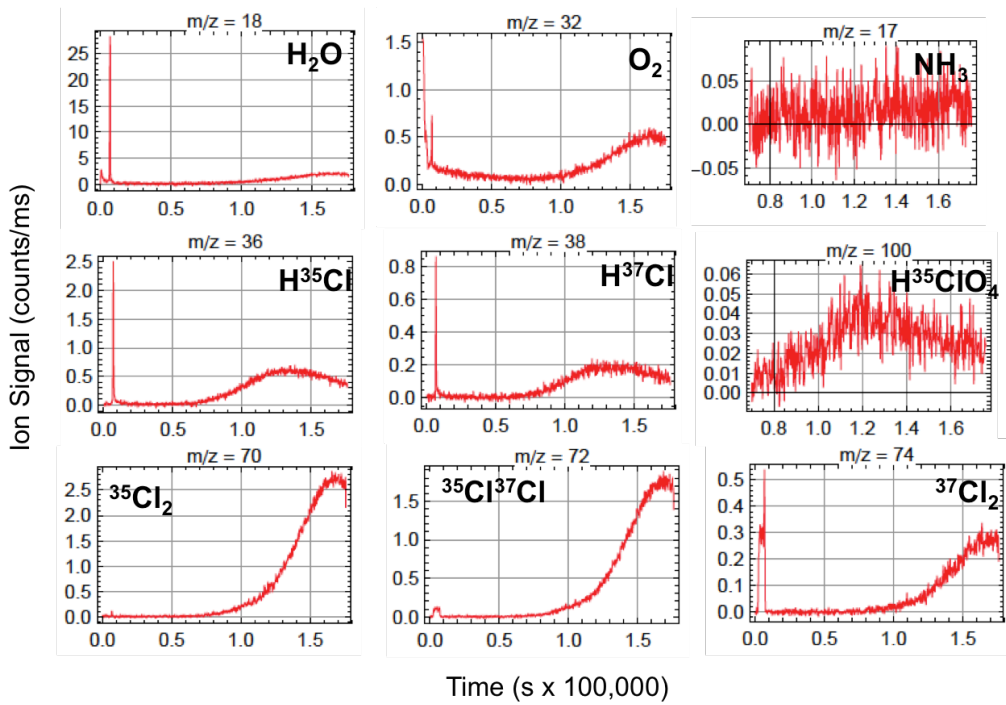


**Figure 12. STMBMS mass spectrum data from isothermal decomposition of AP/RDX mixture at 170°C, showing decomposition products evolved during the later AP reaction step. Slow decomposition of AP occurs after approximately 50,000s, generating NH<sub>3</sub>, HClO<sub>4</sub>, Cl<sub>2</sub>, H<sub>2</sub>O, and O<sub>2</sub>; typical AP decomposition products.**

To determine the onset temperature of this reaction, a series of isothermal STMBMS experiments at varying temperatures were completed. Mass loss data from these experiments are shown in Fig. 13. As the figure shows, the RDX decomposition step occurs after a delay of approximately 6,500s at 170°C, after a delay of 75,000s at 150°C, and does not appear to occur at 135°C within 10 days. The onset temperature of the reaction therefore appears to be between 135-150°C. Importantly, the onset of thermal decomposition of ammonium perchlorate is approximately 130°C [8], further suggesting that decomposition products of ammonium perchlorate may be responsible for initiation of decomposition of RDX in these experiments.

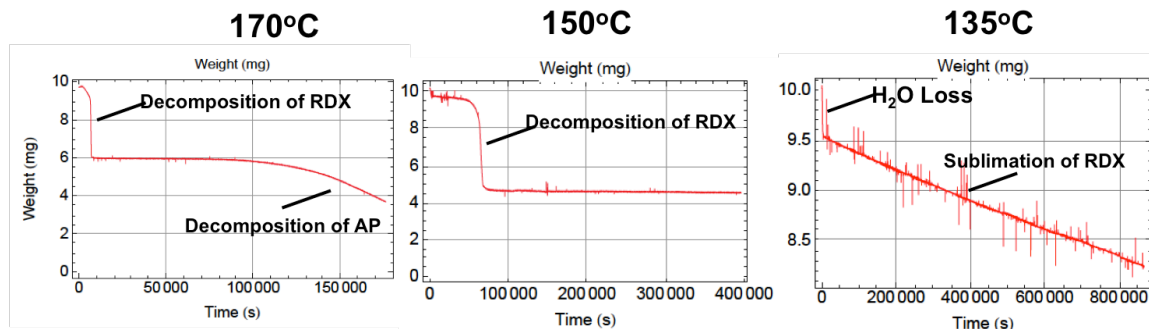


**Figure 13. STMBMS mass loss data from isothermal decomposition of AP/RDX mixtures at 170°C (left), 150°C (middle), and 135°C (right), showing temperature dependence of delayed reaction of RDX. At 170°C, decomposition of RDX occurs at 6,500s. At 150°C, reaction occurs at approximately 75,000s. No reaction is observed after 10 days at 135°C.**

STMBMS data from isothermal decomposition of AP/RDX mixture under very high confinement, produced by loading the sample into a reaction cell with a 5  $\mu\text{m}$  orifice, is shown in Figure 14. With such a narrow orifice, decomposition gases do not escape the reaction cell as quickly, and the reaction proceeds slowly enough that its constituent steps can be observed. Figure 14 shows representative mass spectrum signals observed during the experiment as a function of time. As the figure shows, the decomposition process proceeds in four distinct phases. In the initial phase, beginning at  $\sim$ 2,000s, several species ( $\text{H}_2\text{O}$ , RDX, a species with  $m/z = 43$ ; possibly isocyanic acid, and others not shown) are observed just as the sample reaches  $170^\circ\text{C}$ . A second phase begins at  $\sim$ 6,500s, during which decomposition of RDX accelerates and generates a series of decomposition products, including  $\text{HCN}$  and  $\text{HCl}$ . The decomposition process then accelerates, and in a third stage, a set of products is evolved in a short burst at approximately 10,000s. This third step constitutes the main decomposition step, and observed products include  $\text{N}_2\text{O}$  and  $\text{CH}_2\text{O}$  from decomposition of RDX, as well as a burst of  $\text{HCl}$  and  $\text{ClO}_2$ . In the fourth and final phase of the RDX decomposition process ( $\sim$ 11,000s), a number of mass signals are observed ( $m/z = 73$ , 147, and 149 are shown); the identities of the species that give rise to these signals are not yet definitively known.

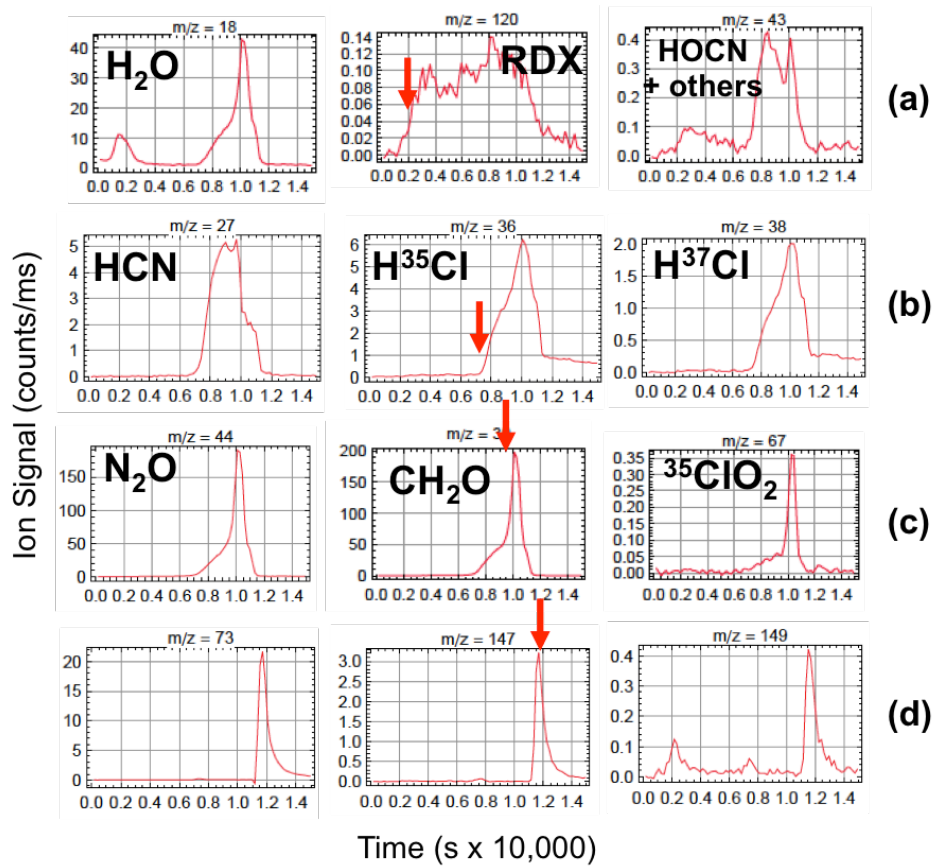


**Figure 14. STMBMS mass spectrum data from isothermal decomposition of AP/RDX mixtures at  $170^\circ\text{C}$  under very high confinement. The reaction proceeds in four distinct phases: (a, top row) initial reactions, (b, second row) beginning of decomposition stage, (c, third row) main decomposition stage, and (d, fourth row) final decomposition stage. Red arrows in the middle column indicate the approximate beginning of each stage of the reaction.**

Given these experimental observations, it is apparent that the observed thermal decomposition of RDX in the presence of AP is initiated by the presence of AP and/or its decomposition products, and RDX subsequently undergoes catalytic (possibly autocatalytic) decomposition. The experimental observations support this conclusion as follows: First, chlorinated products (HCl and ClO<sub>2</sub>) are observed during and are temporally correlated with the RDX decomposition steps, and appear before the ammonium perchlorate has undergone significant decomposition. This confirms that there is a chemical interaction between AP and RDX, as AP is the only source of chlorine atoms in the mixture. Thermal decomposition of ammonium perchlorate produces a number of reactive species that could be responsible for initiating the decomposition process, including HClO<sub>4</sub>, a powerful oxidizer, and NO, which is known to catalyze decomposition of RDX [11]. Second, the ammonium perchlorate is not significantly consumed during the rapid RDX decomposition step. This implies that AP and its decomposition products initiate and/or catalyze the decomposition of RDX, but are not primary reactants in the main decomposition steps. Third, RDX decomposes much more rapidly both above and below its melting point in the presence of AP than it does alone. This acceleration of the decomposition reactions implies that the thermal decomposition process is catalyzed. RDX thermal decomposition is known to be autocatalytic [11]. The fact that the observed decomposition products of this reaction are similar to the known RDX thermal decomposition products suggests that autocatalytic decomposition may be involved. However, it is also possible that the AP and its decomposition products directly catalyze the decomposition of RDX. In either case, it is apparent that AP and/or its decomposition products initiate decomposition of RDX, which then undergoes catalytic decomposition, resulting in complete decomposition of the RDX.

## SUMMARY AND CONCLUSIONS

We have characterized chemical interactions that occur between ammonium perchlorate and RDX at elevated temperatures. In the presence of ammonium perchlorate, RDX undergoes rapid thermal decomposition in a reaction that entirely decomposes the RDX but does not significantly consume the ammonium perchlorate. The reaction is observed to occur at temperatures of 150°C and above, and proceeds more rapidly above the melting point of RDX. The decomposition of RDX in the presence of AP is much faster than the decomposition of RDX alone. The accelerated nature of the reactions, combined with the observation of both chlorinated species and typical RDX decomposition products, implies that AP and/or its decomposition products initiate decomposition of RDX, which subsequently undergoes catalytic decomposition. The catalytic decomposition of RDX in the presence of AP may be autocatalytic (driven by RDX decomposition products) or catalyzed by AP and/or its decomposition products. Future work will characterize the complete thermal decomposition reaction mechanism.

## ACKNOWLEDGMENTS

The authors would like to thank Deneille Weise-Smith and Aaron Highley of Sandia National Laboratories, California, for excellent technical support. The authors also acknowledge Dr. Richard Behrens of Sandia National Laboratories, California, for helpful discussions.

## REFERENCES

1. Kay, J., Biggs, G., Hayden, H., and Babcock, W., "Chemical Changes During Aging of Underwater Explosives", in *proceedings of the 38<sup>th</sup> JANNAF Propellants And Explosives Dev. and Char. Subcc. Meeting*, Charleston, SC, USA, May 2014.
2. Behrens, R., Jr., "New Simultaneous Thermogravimetry and Modulated Molecular Beam

Mass Spectrometry Apparatus for Quantitative Thermal Decomposition Studies", *Rev. Sci. Instrum.* **58**, 451 (1987).

- 3. Behrens, R., Jr., "Identification of HMX Pyrolysis Products by Simultaneous Thermogravimetric Modulated Beam Mass Spectrometry and Time-of-Flight Velocity-Spectra Measurements", *Int. J. Chem. Kin.* **22** 135 (1990).
- 4. Behrens, R., Jr., "Determination of the Rates of Formation of Gaseous Products from the Pyrolysis of HMX by Simultaneous Thermogravimetric Modulated Beam Mass Spectrometry", *Int. J. Chem. Kin.* **22** 159 (1990).
- 5. Behrens, R., "Thermal Decomposition Processes of Energetic Materials in the Condensed Phase at Low and Moderate Temperatures." In *Overviews of Recent Research on Energetic Materials*, Shaw, R. W.; Brill, T. B.; Thompson, D. L., Eds. World Scientific Publishing Co.: Singapore, 2005; pp 29 - 74.
- 6. Minier, L., Behrens, R., Jr., "A Study of the Solid-Phase Thermal Decomposition of NTO Using Simultaneous Thermogravimetric Modulated Beam Mass Spectrometry (STMBMS)", in *proceedings of the 33<sup>rd</sup> JANNAF Comb. Subcc. Meeting*, Monterey, CA., USA, Nov. 1996.
- 7. Atwood, A.I., Ford, K.P., Curran, P.O., Lyle, T.M., Wheeler, C.J., Daniels, A., "Prediction of IM Response and Small Scale Tests", Presented at *TTCP Workshop, DSTL*, Halstead, UK, March, 2009.
- 8. Boldyrev, V. V., "Thermal Decomposition of Ammonium Perchlorate", *Thermochimica Acta* **443** (2006) 1-36.
- 9. Behrens, R. and Bulusu, S., "Thermal Decomposition of Energetic Materials. 3. Temporal Behaviors of the Rates of Formation of the Gaseous Pyrolysis Products from Condensed-Phase Decomposition of 1,3,5-Trinitrohexahydro-s-triazine (RDX)". *J. Phys. Chem.* **1992**, *96*, 8877-8891.
- 10. Behrens, R. and Bulusu, S., "Thermal Decomposition of Energetic Materials. 4. Deuterium Isotope Effects and Isotopic Scrambling in Condensed-Phase Decomposition of 1,3,5-Trinitrohexahydro-s-triazine (RDX)". *J. Phys. Chem.* **1992**, *96*, 8891-8897.
- 11. Maharrey, S. and Behrens, R. "Thermal Decomposition of Energetic Materials. 5. Reaction Processes of 1,3,5-Trinitrohexahydro-s-triazine (RDX) below its Melting Point". *J. Phys. Chem. A* **2005**, *109*, 11236-11249.